Multidisciplinary Process Integration and Design Optimization of a Hybrid Marine Power System Applied to a VLCC

Sabah Alwan, NTNU, Trondheim/Norway, sabah.alwan@ntnu.no
Kevin Koosup Yum, SINTEF Ocean, Trondheim/Norway, KevinKoosup.Yum@sintef.no
Sverre Steen, NTNU, Trondheim/Norway, sverre.steen@ntnu.no
Eilif Pedersen, NTNU, Trondheim/Norway, eilif.pedersen@ntnu.no

Abstract

In this paper, we explore the use of multidisciplinary and high-fidelity simulations for multi-objective design optimization of a marine hybrid propulsion system with application to a very large crude oil carrier (VLCC) tanker. The optimization is achieved by utilizing a process integration and design optimization (PIDO) to support multidisciplinary design optimization (MDO). We performed a minimum number of simulations to explore the design space through algorithm-guided design-of-experiments (DoE). Based on those experiments, response surface models (RSMs) were constructed. Further, sensitivity and correlation within design parameters and with the design objectives from the simulations are simultaneously examined and elucidated. Subsequently, the quality of the RSMs is validated using the simulation models. A multi-objective optimization is then carried out by utilizing the RSMs rather than the high-fidelity simulation. Standard particle swarm optimization (sPSO) was used with the RSMs while a very large number of design variation and alternatives are swiftly examined. Remaining work is to test optimal design solutions for their reliability and robustness through sensitivity to changes in operational requirements, changes in environmental conditions and imprecision in design parameters.

1. Introduction

A ship is a complex system in which many designers develop and consider different aspects of the system to meet various functional requirements. Traditionally design decisions are made in two different levels, that is a system level and a component level. In the system level, often the optimization objective is to make the ship as economic as possible, whereas in the component level, the objective is to meet the component's solitary functional requirements within the given constraints. In this paper, we hope to shed light on the use of an integrated multidisciplinary simulation-based framework for multi-objective design optimization of a vessel system performance rather than component based design and optimization. These approaches are recently and widely in use within the aerospace and automotive industries alike *Frenzel, Heiserer et al. (2015)* and *Van der Auweraer, Donders et al. (2008)*, with lesser usage in the maritime industry where its often discipline specific *Liu and Collette (2014)* and *Parsopoulos and Vrahatis (2002)*. Using a well-established approach from other industries can potentially improve design outcomes *de Weck, Agte et al. (2007)* by simultaneously considering different aspects of the system. Therefore, process integration and design optimization (PIDO) tools are used to support multidisciplinary design optimization (MDO). In MDO, a metamodel is often derived from performing a minimum number of multidisciplinary system simulations guided by smart algorithm such as Latin Hypercube *Eglajs and Audze (1977)* or Factorial Design *Box and Hunter (1961)* through design-of-experiment (DoE). In the system simulation, several domain specific virtual models and processes are interlinked in accordance with the design task. In this paper, models include ship operational model, metocean models, ship hydrodynamics, propulsion, electrical load and powering models to simulate the total system performances. The metamodel can be in the form of a response surface model (RSM) *Box and Wilson (1992)* that is constructed by a polynomial, support vector machine (SVM) for supervised machine learning, a neural network, Kriging, etc. Subsequently, multi-objective optimization is achieved by the utilization of the metamodel and varying design parameters with optimization algorithms within some design constraints to achieve certain performance objectives. Several optimization algorithms were tested and found to vary in their performance and convergence.
In this paper, we present an application of MDO using a PIDO platform for the design of a hybrid

marine power plant for a VLCC. In the power plant, the main engine drives the propeller shaft as in the conventional system, and the power take-in (PTI) / power take-off (PTO) device is used to harvest or boost power to the propeller shaft. To maximize the capacity of the PTI/PTO device with minimal influence on the electrical power plant, an energy storage system such as battery pack or a super-capacitor bank is used. The aims of this particular configuration are: (1) to reduce the fuel consumption in low load operation by reducing the main engine power without losing extra propulsion power for rough weather, and (2) to enhance the dynamic response of the propulsion system, reducing the fluctuation of the propeller speed and, thus, the chance of over-speeding. The numerical simulation provides the average fuel consumption for the given probabilistic operational conditions from weather and speed, and the dynamic response of the system in time-series. The goal of the optimization is to find the best configuration of the main components in terms of capacity to achieve the minimum fuel consumption. The capacities of the components in question are those for the main engine, the PTI/PTO device, the auxiliary engine, and the battery. This paper includes a description of MDO method and discusses the applicability and challenges in ship design. Uncertainties related to operational condition and system design variables and parameters were examined to achieve the required level of system reliability and efficiency. A MDO case study of a tanker operating in adverse condition is presented.

2. Process Integration and Design Optimization

Four main objectives behind Process Integration and Design Optimization (PIDO) tools are to create an automated design process, design space exploration, design optimization and ultimately design for value robustness. In process automation, separate engineering disciplines can be integrated for better design performance evaluation and reducing repetitive design tasks, development time, and trail & error. Designers can perform and evaluate multiple designs simultaneously by exploiting the rapid increase in computational power and parallel processing. Also, explore the design space methodically by investigating large numbers of possible design alternatives and employing specialized search algorithm on different design combination. Visualize and analyze statistically various design parameters relations through sensitivity analysis, screening and intelligent sampling.

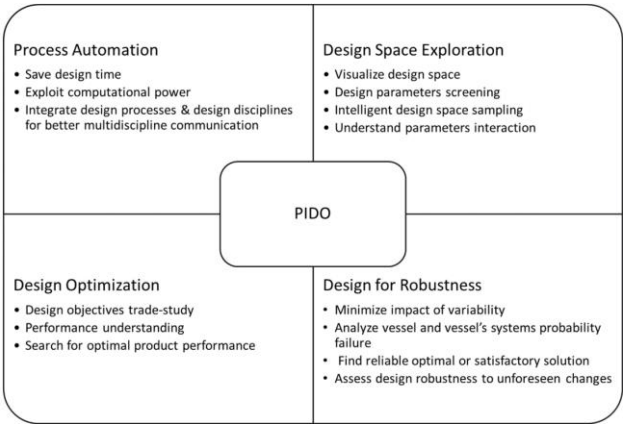

Fig.1: Diagram explaining the underlying rationale behind PIDO

Results from various simulations are then used in machine-learning or to construct RSMs. These models are then cross validated against or validated against few high-fidelity simulations, and then used as independent models for design optimization. Optimization is then carried out using global search evolutionary algorithm such as (MOGA, sPSO) for the first stage and gradient based algorithm for the final stage. Final optimal design configurations are then verified with the high-fidelity simulation.

Most of the aforementioned statistical methods, integration of processes from different disciplines and optimization are known in various scientific and engineering disciplines, however they are challenging to apply into practical ship design tasks due to difficulties in auto-generation and evaluation of precise design alternatives such as hull-form and propeller, or scaling the size of main engine and generators

without careful considerations. These difficulties by no means depreciate the value and progress made by various tools for modeling and analyzing ship's subsystems. Furthermore, the nature of ship design means that design requirements, objectives and constraints often change during the design process based on new observations and results interpretations *Andrews (2004)* and *Gero and Kannengiesser (2004).* Lastly, there is a level of challenges that arises from communicating data between different design disciplines and the nature of the information flow. For instance, there is no specific format or approach or boundaries where one subsystem and its requirements and constraint can interact with the next subsystem with its objectives and constraints. That being said, theoretically challenges can be reformulated into opportunities where constraints can be shared and softened among subsystems or turned into objectives.

Essentially PIDO philosophy tries to bring about wider systematic design perspective, to utilize various statistical methods as aid tools in the design process, to improve on computational cost through smart experimentation, provide more precise models from simulation data with lower uncertainty instead of relying exclusively on approximate heuristic models, and finally to enable designers to consider wider system boundary at an early design stage.

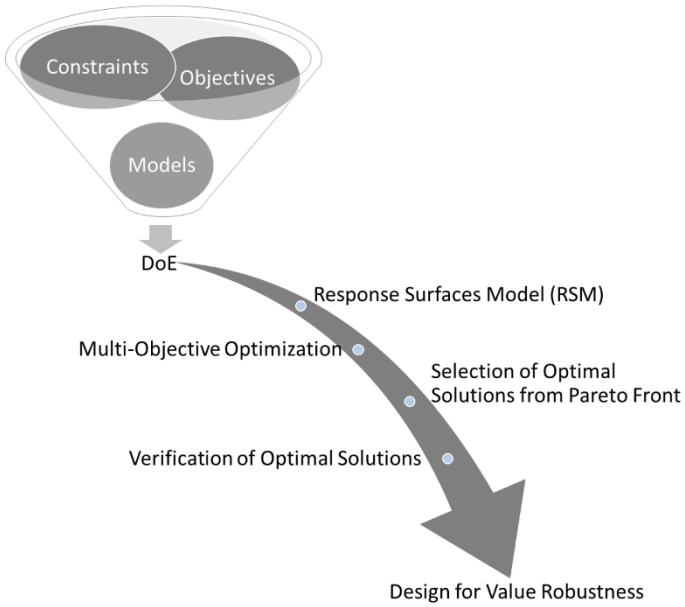

Fig.2: PIDO process follows from design models-constraints (hard/soft)-objectives to formal DoE study. RSM and/or supervised machine learning model is then constructed and validated with the initial models. Optimization is then carried out using suitable algorithm to examine large number of design alternatives. Optimal results are then verified with the initial models and tested for their robustness.

3. Simulation Models and Workflow:

The PIDO workflow utilizes machinery models and ship hydrodynamic aspects as proposed in *Yum, Skjong et al. (2016), Yum, Taskar et al. (2016)* as well as ship voyage simulation model for weather and transporter capacity. The PIDO workflow is based on Noesis Solutions Optimus software tool. This workflow essentially guides the simulation models and their parameters, and extract results for each run, then store and re-use knowledge acquired during each simulation including trends and relationships that lead to specific solutions.

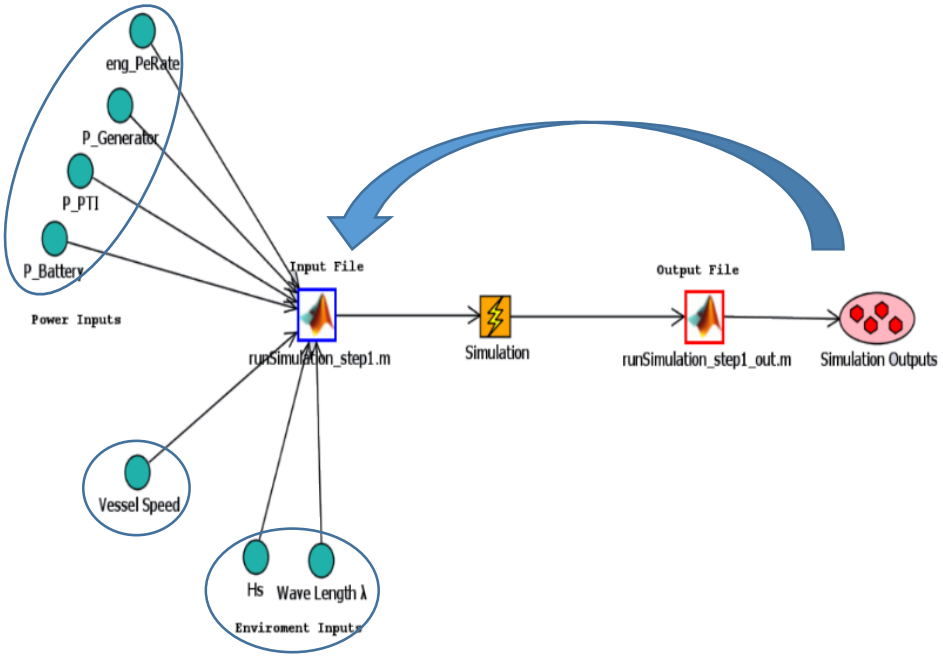

Fig.3: Simulation workflow that perform the virtual vessel design optimization (Created with Noesis Solutions Optimus software tool)

The vessel model in use based on the well-known KVLCC2 model where vessel particulars can be found in the appendix. Hydrodynamic coefficients were computed using the ShipX Veres module from SINTEF Ocean, which is using linear strip-theory *Salvesen, Tuck et al. (1970)* to compute the vessel motions. The added resistance is then computed according to the modified version of Gerritsma & Beukelmans as presented in *Loukakis and Sclavounos (1978)*. The ship propeller was based on the modified propeller design and open water propeller diagrams and wake estimation procedure as proposed in *Taskar, Yum et al. (2016), Yum, Skjong et al. (2016)*. Pre-processing simulation is then carried out and stored in a database for both regular and irregular waves with Hs (significant wave height) and T_p (peak period) according to the metocean model outputs.

The structure of the machinery and propulsion simulation model is presented in Fig.4, which only provides the model structure in the component levels. In addition to the component models, controllers such as an engine governor, a governor for PTI/PTO device and a power management system had been implemented order to run the dynamic simulations for different operating conditions. *Table I* shows the modeling framework used for the submodels.

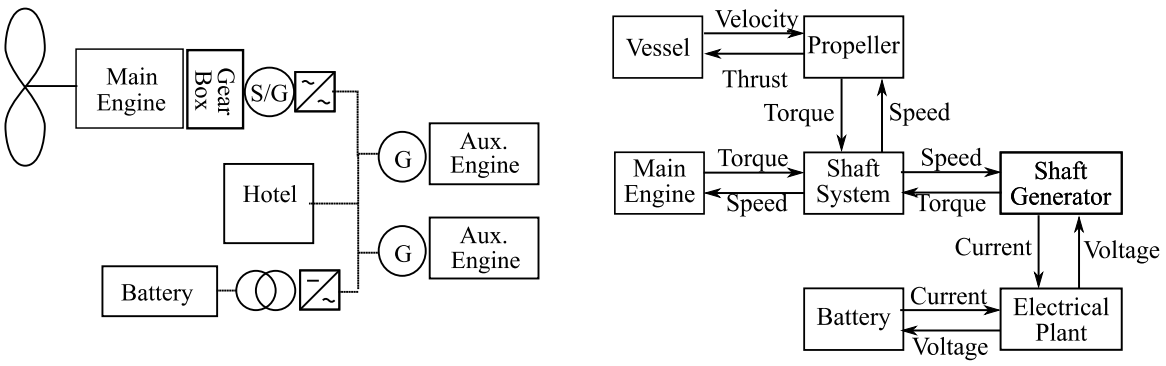

(a) Hybrid propulsion system (b) System model

Fig.4 Schematic of the hybrid propulsion system and the structure of the simulation model

Table I: Modeling framework of the submodels

Submodel	Modeling framework	Submodel	Modeling framework
Electrical system	Dynamic model using dq-frame	Shaft system	Single rigid-body
Diesel engine system	Filling and emptying method 0D phenomenological combustion	Vessel	1D rigid-body Calm Water Resistance Curve Added Resistance Coefficient
Battery system	Capacitance and resistance model	Propeller	Quasi-steady based on propeller curve Mean wake variation model Ventilation model

However, the models had to be modified in order to be used in the design space exploration to overcome the two challenges: simulation time and robustness of simulation over various configurations of the power plant and operational conditions.

The average simulation time for the hybrid propulsion system in the previous work was typically 10~15 times slower than real time when the whole system was run as a single simulation on a high-performance computer. The main reason for the slow computational speed was to include both the electrical models and the diesel engine models that have very different time scales. Co-simulation could enhance the computational speed but not so drastically. In this regard, we decided to divide the simulations into three where the second and third part of the simulation is carried out in sequence. First, the vessel transport capacity is simulated for a given logistical network where vessel speed and carrying capacity are estimated, then metocean data from hindcast along the sailing route are computed into probabilities of occurrence and communicated to the rest of the simulation as an input. The second part of the simulation is the mechanical system which includes the coupled hull-propeller-machinery system. This is run first and the logged signals from the simulation are provided as inputs to the electrical system simulation. The interface between the second and third parts of the simulation is the PTI/PTO, which is modeled by a first-order transfer function in the mechanical simulation whereas it is modeled by its first principle physics model. The structure of the revised simulation model is presented in *Fig.5*. As a result of changing from the simultaneous simulation to the sequential one, the simulation runs approximately 30% faster than real time. Note that the electrical simulation is skipped in case that the PTI/PTO device provides enough electricity for the auxiliary loads so that the generators do not need to run.

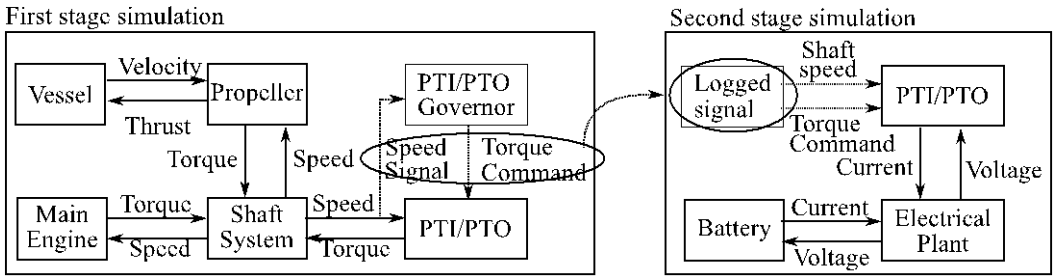

Fig.5: The revised structure of the simulation model

Regarding robustness of the simulation, the capability of the controllers had to be extended to enable the various operational modes depending on the power loads. The control objective of the PTI governor in the previous work was to regulate the shaft speed with minimum fluctuation for propulsion in waves. However, in order to simulate the performance in both the PTI and PTO mode, the mean power load on the shaft is to be shared between the main engine and the PTI/PTO device depending on the available power and the level of the power load. The control objectives for the PTI/PTO device for different powering modes are:

PTI mode ($P_{ME,Max} < \overline{P}_{Prop}$): While keeping the shaft speed constant, the device should provide the power to the shaft as much as possible so that the main engine does not operate above the torque limit

for the given shaft speed.
PTO mode ($P_{ME,Max} > \overline{P}_{Prop}$): While keeping the shaft speed constant, the device should take off enough power from the shaft to provide the auxiliary loads. The torque of the main engine should be kept within the limit in any case.

It is however difficult to interfere the simulation manually as the number of simulations for the design study is too large for that. Introducing switching controllers depending on the mode may lead to instability in simulations for many combinations of different parameter sets. In order to tackle this challenge, we introduced load limiting droop control for the sharing loads between the main engine and the PTI/PTO device.

In general, a droop control is used for sharing the loads between the generators running in parallel. When the same droop curve is applied between two powering units, they share the load proportional to their rated power. This proportion can be regulated either by changing the slope of the curve or changing the reference frequency at no load. Usually the droop curve is defined for the power between 0 and 100%, but we defined the droop between -50 to 50% as PTI/PTO device can either be powering (positive power) or being powered (negative power). The droop curve for the main engine and the PTI/PTO device is shown in Fig.6. When the reference speed is given to the governors, it is multiplied by the value of the droop curve depending on the load to give the set point to the speed controller. From the defined droop curve in *Fig.6* for an identical speed reference, PTI/PTO will share the load of 20% of its capacity when the main engine is running at 70% load, or -20% of its capacity when the main engine is running at 30% load. The corresponding droop values are 0.99 and 1.01, respectively. The curve for the PTI/PTO device is flat outside the range because some power should be reserved for smoothing the power and speed fluctuations during propulsion in waves.

Furthermore, the proportions of load sharing can be adjusted by increasing or decreasing the speed reference value to one of the devices, which has the effect of lifting or lowering the droop curve of the device. As the speed reference is increased, the device has to work harder than the other that is controlled at the original reference, and vice versa. As shown Fig.6, when the speed reference for PTI/PTO is increased by a certain value, 1.5% in this case, the dotted line represents the new set point. In this case, while the main engine is running 70% of its power, the PTI/PTO will provide 50% of its rated power to the shaft, 30% increase compared to the identical set point in Fig.7. In the opposite case, decreasing the reference value by 1.5%, PTI/PTO will take off 50% of its rated power from the shaft while the main engine is running at 30%.

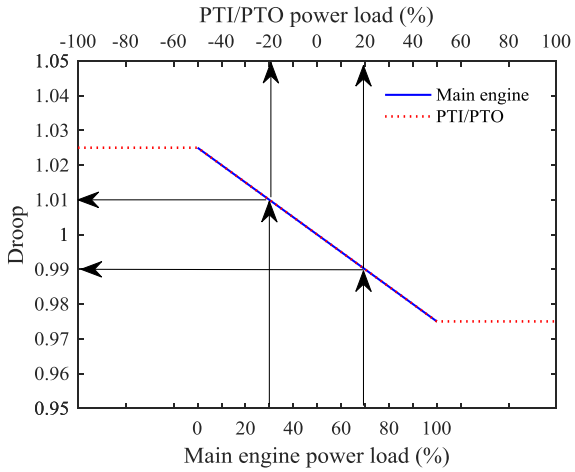

Fig.6: Droop curves for the main engine and the PTI/PTO

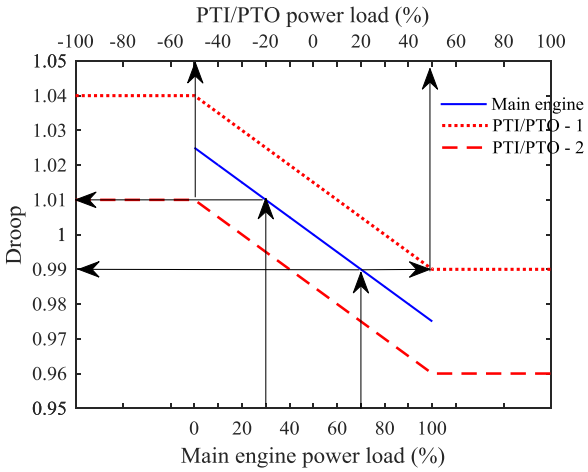

Fig.7: Adjusting the load sharing proportion by changing the speed

Using the principle above, the load sharing of the main engine and PTI/PTO can be controlled by adjusting the speed reference to the governor for PTI/PTO. This is achieved by the controller presented

in Fig.8. PTI load control is the only active controller that regulates the load sharing. In case that maximum allowable engine load smaller than the average propulsion load ($P_{ME,Max} < \overline{P}_{Prop}$), which will be represented by the engine governor output greater than 1, PTI load control will give negative value so that the speed reference for the PTI/PTO device will increase, thereby, increasing the power load. In the other case, $P_{ME,Max} > \overline{P}_{Prop}$, the speed reference will decrease, reducing the power load and entering PTO mode eventually. However, the average power production from PTO mode should not exceed the power demand of the auxiliary loads. Therefore, if the average power production is greater than a certain portion of the auxiliary power demand, the PTO load controller becomes active which controls the power load of PTO to match the auxiliary power demand while the PTI load controller becomes inactive. The transition from PTI load control to PTO load control happens through the hysteresis type of switching so that they do not swing back and forth. This controller proved to be robust for all the variations of parameters and the operational conditions during the simulation.

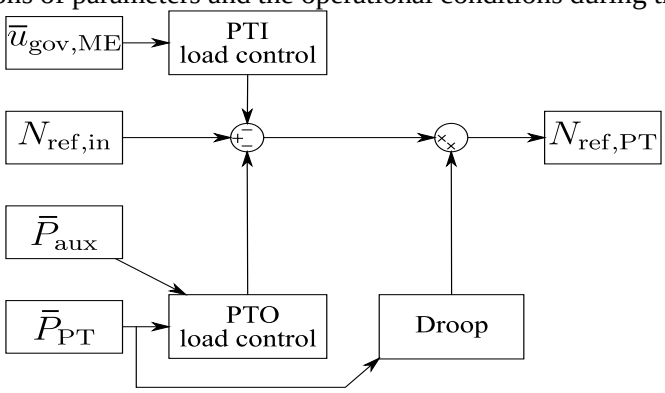

Fig.8: Schematic of PTI/PTO load sharing control

In addition to the operational variations in the simulation, the simulation models also have to cope with variations of the parameters in a large range for the design study. As most of the models are based on the first principles, there are large sets of parameters to be changed along the design parameters. It will be impossible to validate the models for each set of parameters in the process of performing design of experiments or optimization. To resolve this challenge, we decided to use the well-validated model and the parameters as is, and convert the power input/outputs only. For example, the interface with between the shaft model and the main engine model includes the information of the shaft and the torque. We assume the shaft speed will not be scaled as the propeller design remains the same, but the torque will be according to the ratio of the rated power of the new design to the original so that the power is properly scaled. The same will be applied for the gensets, batteries and PTI/PTO device.

4. Case Study: Environmental condition, operational profile and design constraints

4.1 Objective

This demonstration case based on the well-known KVLCC2 operating in adverse weather condition. The vessel's particulars, propeller characteristics and the machinery are provided in *Yum, Skjong et al. (2016), Yum, Taskar et al. (2016).* The objective of the optimization study is to find the set of the design parameters for capacity of the machineries that gives the minimum fuel consumption per miles for the given probabilistic operational scenarios (weather and speed) are calculated.

The particular values are for the nominal design where the parameters in *Table II*. will vary for the design space exploration and optimization. In addition to the high and low limit for the parameters, it must meet other constraints in order to ensure enough power for the propulsion and the auxiliary power.

$$P_{PT} + P_{ME} \geq P_{PropReq}$$

$$P_{Gen} \geq \frac{(P_{PropReq} - P_{ME} + P_{Aux})}{2\eta_{Gen}}$$

where, $P_{PropReq}$ is a minimum power requirement for the vessel to survive under harsh weather and P_{Aux} is the auxiliary power load. In this study, they are assumed to be 25MW and 1MW, respectively.

Table II: Design parameters and their constraints

	Description	Range	Remark
P_{PT}	Rated power of the PTI/PTO	0 ~ 8MW	The same rate for PTI and PTO
P_{ME}	Rated power of the diesel engine	17.5 ~ 25MW	
P_{Batt}	Rated power of the battery	0 ~ 5 MW	The same rate for charging and discharging
P_{Gen}	Rated power of the genset	1.15 ~ 4.8 MW	

4.2 Operational profile

An evaluation of vessel speed to meet transport capacity and sailing through calm-to-rough weather conditions in the Northern Atlantic Ocean were performed with event-based voyage simulation. Results from this model were expressed in the form of probability distributions for equivalent Hs and vessel speed. The environmental conditions are stochastically independent while the vessel speed is a stochastic parameter influenced by markets from supply and demand between portal cities, and influenced by the environmental condition during voyage where voluntary speed reduction deemed necessary.

The probability of the equivalent wave condition along the sailing route P(W) is stochastically independent based on sample mean, rather than population mean, from hindcast open source weather data. Rationally, the vessel operating speed is a conditional probability. For a better speed and transport capacity estimation the vessel's maximum possible attainable speed can be pre-determined for a given weather condition and formulated in the below equation considering involuntary speed reduction from *Table 5* where T_p is the peak wave period and Hs is the significant wave height.

$$P(V \cap W) = P(V|W)P(W) \qquad (1)$$

Probabilistic operational profiles for vessel speeds (9, 11, 13 and 15 kts) and encountered environmental conditions (0, 1, 2, 3 and 4 m) for the sailing route were presented in 3 weather scenarios and 4 speeds as shown in Tables III and IV.

Table III: Five weather conditions with different frequency of occurrence from hindcast data along the sailing route.

Hs	Scenario 1	Scenario 3	Scenario 3
0 m	5%	5%	5%
1 m	10%	10%	12%
2 m	10%	20%	45%
3 m	55%	55%	28%
4 m	20%	10%	10%

Table IV: Combination of speeds with their frequency of occurrence to satisfy transport requirement.

Speed [kts]	Frequency Speed
9	15%
11	50%
13	20%
15	15%

Table V: Maximum attainable speed based on ship hydrodynamic calculation for different Hs & T_p.

Hs|T_p	5.66	8.00	9.80	11.32	12.65	13.86	14.97	16.01	16.98	17.90
1	14.97	14.96	14.96	14.95	0.00	0.00	0.00	0.00	0.00	0.00
2	14.99	14.96	14.90	14.57	14.45	14.35	0.00	0.00	0.00	0.00
3	0.00	14.54	13.47	12.52	12.33	12.09	11.88	11.97	0.00	0.00
4	0.00	0.00	0.00	9.63	9.25	8.84	8.54	8.85	9.15	9.44
5	0.00	0.00	0.00	0.00	0.00	4.47	4.42	5.04	5.59	6.37

4.3 Design of Experiment (DoE)

Design of experiment (DoE) was performed for each discrete operational point (combination of speeds and weather conditions) by sampling the list of design parameters from *Table 2* with Latin Hyper Cube Sampling technique. A total of 216 near-random experiments were produced for each operating point to explore the entire design space. Each evaluation of design combination is independent and therefore possible to carry out the simulation in parallel. In the DoE, we aimed at finding the influence of design parameters (inputs to the simulation) at the output response in terms of fuel consumption, torque and RPM fluctuation), which are the most dominant design parameters and at which condition, and finally how to predict outputs based on any set of design inputs. Correlation scatter matrices and bubble plots as presented later in results sections are used to screen out the least important design parameters and thus to focus the optimization resources on the most important parameters.

4.3.1 Response Surface Model

Using the results from LHC, a response surface model for each output is constructed. We used support vector machines (SVM) as a regression function that maps the inputs of design parameters to the output *Brereton and Lloyd (2010)*. While building the SVM models, it was found that the number of generators in operation causes some of our key outputs to be discontinuous. Therefore, the number of generators running that is an output of the simulation should be used as an input to estimate these outputs. Therefore, two layers of SVMs are used. Support Vector Machine classification (SVC) model was constructed to classify whether the inputs result in 0, 1 or 2 gensets in operation. Then a Support Vector Machine for regression (SVR) model was constructed to perform regression analysis and predict values of the continuous variables. The aim of this combined SVM is to provide a good prediction of fuel consumption per mile (SFCPM) for any combination of P_{ME}, P_{PT}, P_{Gen} and P_{Batt} as shown in Fig.9.

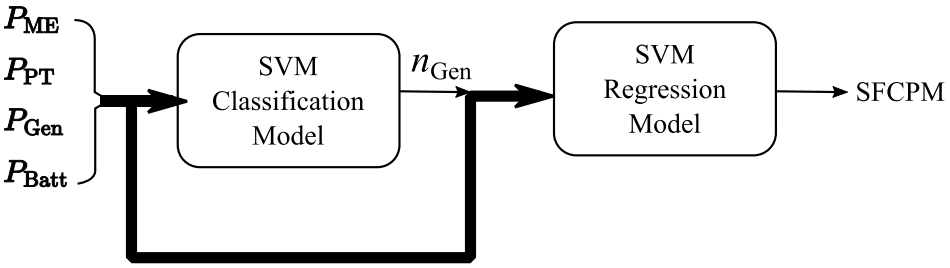

Fig.9: Schematic diagram for 2 levels SVC and SVR models constructed after the DoE study

Bayesian based optimization algorithm was used for training of the SVM parameters to get the best fit of the model. Lastly, cross-validation was performed using the dataset that is not used in the training in order to validate the SVMs for its generality. *Fig.10*, (A, B and C) show strong agreement between predicted SFCPM and computed (Reference) SFCPM from 3 different scenarios of weather condition and vessel speed.

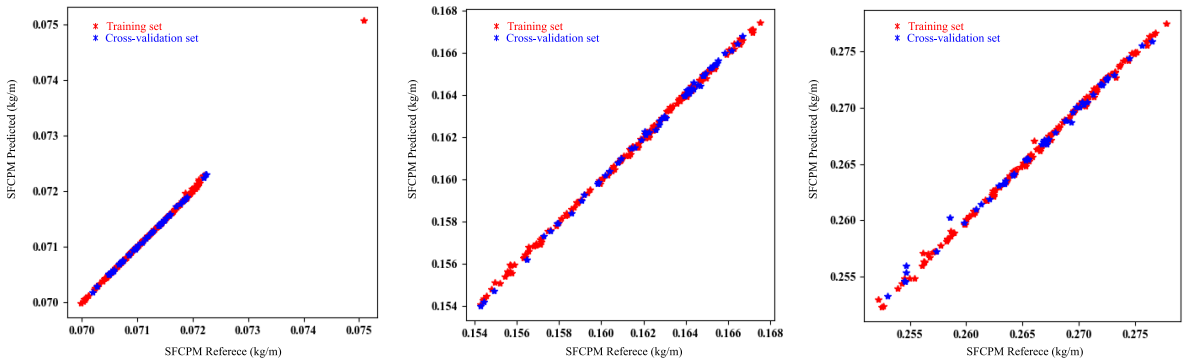

(a) Vs 11kts, Hs 0m (b) Vs 15kts, Hs 2m (a) Vs 11kts, Hs 4m

Fig.10: Validation results from 3 randomly selected weather and speed scenarios

4.4 Study Scenarios

The main objective function of this case is to reduce the overall fuel consumption per miles for the given operational and weather conditions while taking into account the vessel dynamic response and feasibility of the machinery configuration. The focus was on finding the best configuration of the main engine, the PTI/PTO device, the auxiliary engine, and the battery where average fuel consumption per nautical mile for the given probabilistic operational scenarios (weather and speed) becomes minimum. The below equation of the objective function is used for consideration of the weather and sailing speed on the vessel's fuel consumption per mile.

$$Objective\ Function = \sum_{i=1}^{n} P_{v,i} \cdot \sum_{j=1}^{m} P_{w,j} \cdot SFC\ per\ mile\ _{(i,j)}$$

Where:

P_v is the probability of the vessel sailing at particular speed.
P_w is the probability of the vessel encountering particular weather condition.

A base vessel was provided with conventional propulsion and powering systems. An optimization problem is formulated based on the 3 scenarios as given in *Fig.11*. A comparison based on attainable speed and wave height was made, and therefore the objective function can be formulated with the assumption of two stochastically independent probabilities for the same attainable speeds and encountered wave height.

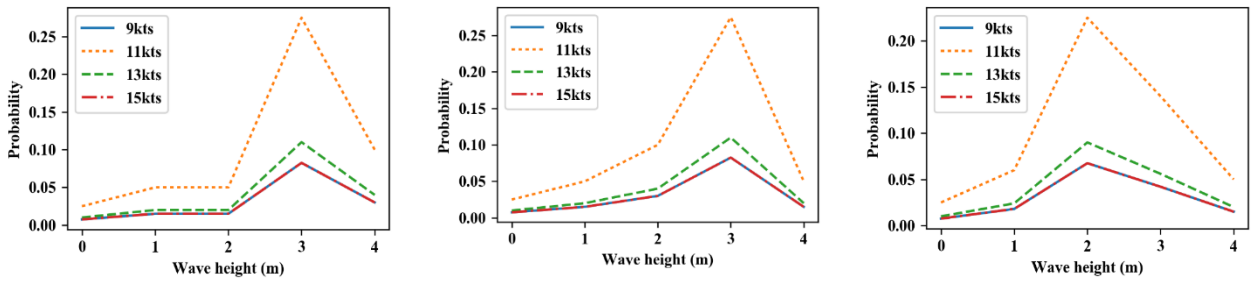

Case 1 Case 2 Case 3

Fig.11: 3 different probabilistic speed and wave height scenarios computed from voyage simulation at the sailing route in Northern Atlantic. Reference data are in Tables III and IV.

Combined optimization algorithms were used where global search algorithm finds the global minima, this was achieved using particle swarm optimization (PSO), and then local search was performed with Gradient Descent method. Both algorithms have their own advantage in finding the optimal solution and their own usage and convergence requirement. It was noted that PSO can find global solution but had difficulties in finding local minima. Gradient descent on the other hand was able to find only local minima and converge rather fast, therefore it required the assistance of other algorithm or multiple starting points in order to find global optimal solution.

5. Results and Discussion

In the first section of the results, the result from the simulations with various sets of design parameters are presented. 216 design sets were sampled for each condition of 20 combined cases of weather and speeds and simulated using the models presented in section 3. From the 20 cases a single correlation matrix is presented for a selected weather condition and operational speed (Hs = 1m and Vs = 15knt) as shown in *Fig.12*. Correlation matrices are used to find relationships between indirectly related design parameters and objectives. From *Fig.12*, it is evident that some parameters are highly correlated (+/-) while some are not. Many interesting hypothesis can be derived, for instance, SFCPM (kg/m) shows strong correlation with most design parameters and outputs with exception of P_{Batt}. This is vastly due

to batteries are used for reserved power storage and damping speed fluctuation rather than fuel saving per se. Fuel reduction due to running the main engine at a more stable load is negligible in these simulations. As the value of SFCPM decreases, propulsion efficiency, P_{ME} increases with negative slope relationship. Also, it can be observed that SFCPM has discontinuities with all inputs and outputs due to switching between having a single generator and not having a generator in operation (PTO mode).

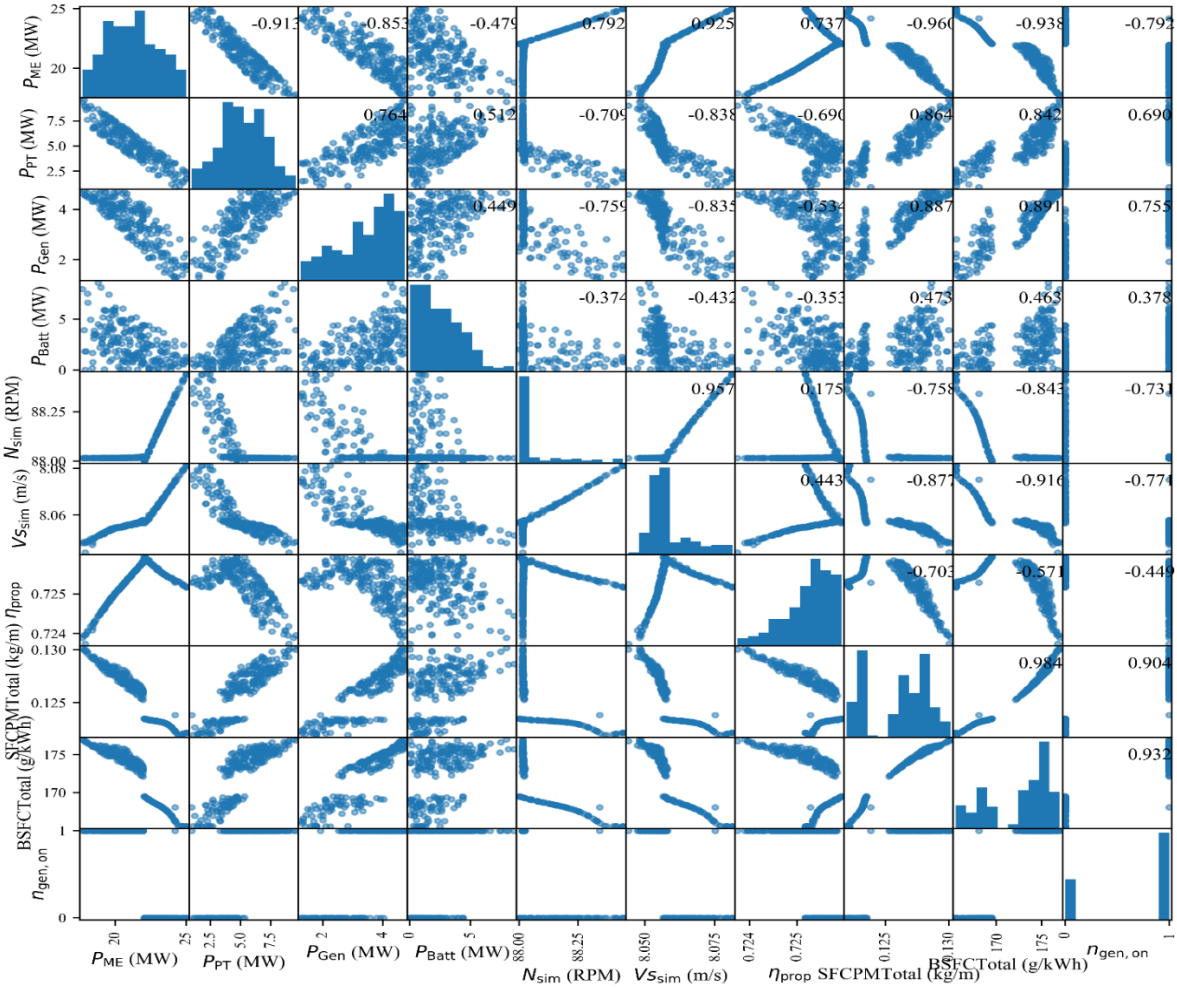

Fig.12. Scatter and correlation matrix for speed of 15 kts and Hs 1 m, generated from 216 high fidelity parallel simulations. Each box contain scatter which represents corresponding values (experimental set) between 2 parameters while the numerical values within the boxes represent the correlation coefficient of the two parameters calculated from the experimental set.

Further data visualization and analysis was performed on combination of design parameters with the system dynamic response and the vessel fuel consumption as shown in *Fig.13*. For this investigation, two sets of speeds at one weather condition was chosen [Vs 15 & 11 kts, Hs 1m]. This is also associated with discontinuities in experimental results in *Fig.13* [A & C]. In these cases, smaller main engine size is associated with higher SFCPM and lower RPM fluctuation. With reduction in vessel speed for the same environmental condition [B & D], results indicate that RPM fluctuation is rather constant for different values of P_{ME} and P_{Gen}, unless P_{Batt} is substantially reduced (small bubbles). Also, for this speed case and weather condition, fuel consumption is solely depending on P_{ME}. Note that the slopes for SFCPM for different speeds [C & D] are opposing each other. This is mainly because of the shape of the fuel consumption curve and the difference in the percentage load in two cases. In [C], the required propulsion power is higher than the main engines are highly loaded where the fuel consumption curve has positive slope. On the other hand, the required power is so low that the engine is loaded where the slope of fuel curve is negative. We can infer that the efficiency of the main engine is a main contributor to the overall system efficiency in a given ship design and the operation condition.

PBatt has rather low correlation values and does not exhibit any relation in the scatter plots with all important design parameters and objectives for this particular operational scenario. This means that it is safe to excluded PBatt from further parameter variation.

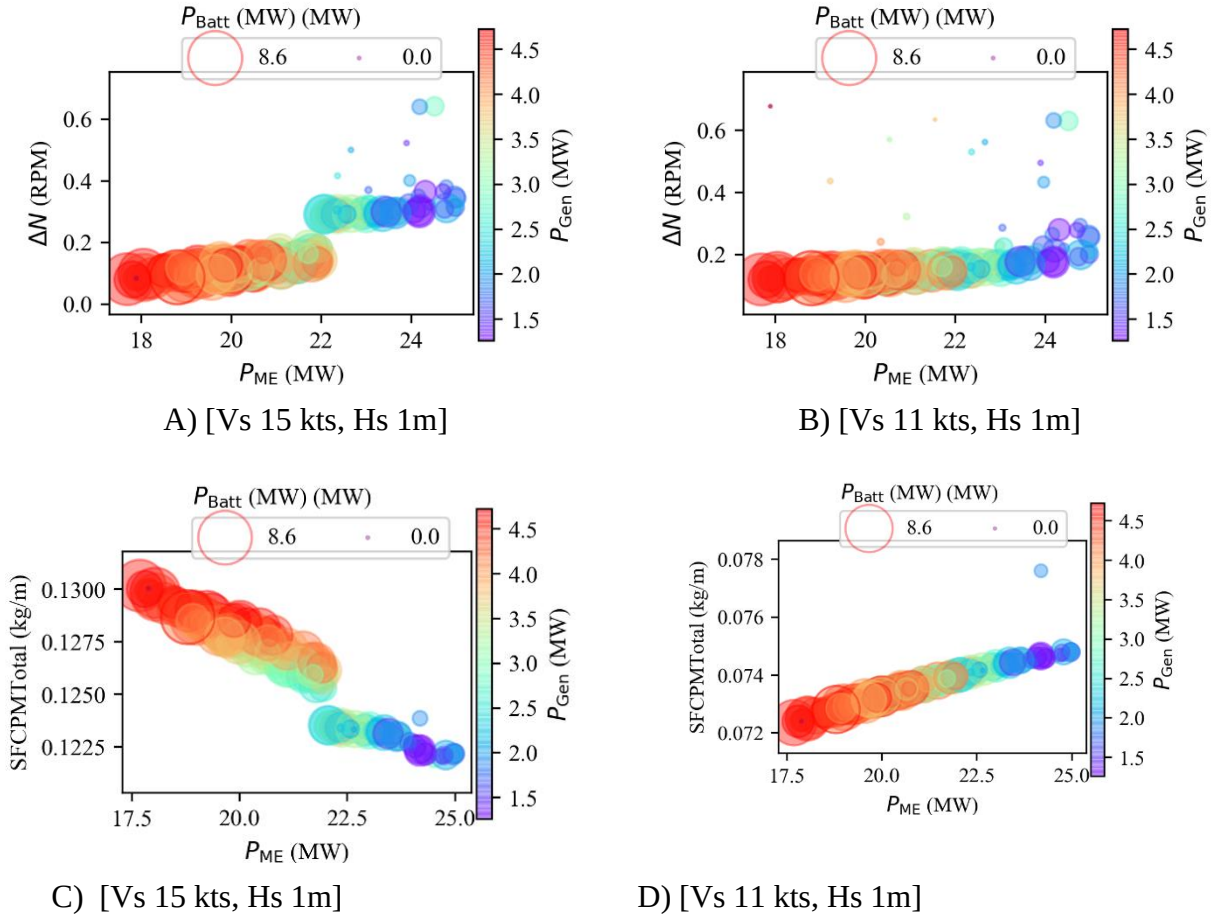

A) [Vs 15 kts, Hs 1m]

B) [Vs 11 kts, Hs 1m]

C) [Vs 15 kts, Hs 1m]

D) [Vs 11 kts, Hs 1m]

Fig.13: Bubble plots show relationship between 3 design parameters and 1 design objective. Parameters are SFCPM, PMe, PBat and generator rating.

Lastly, optimization results from the combined weather condition and vessel speed are presented in Table 6. Counterintuitively that case 3 where the vessel experience less severe weather and sails at the same speed benefits the most from the optimization. After the optimization, the obtained design parameters were verified against the high-fidelity simulation as presented in *Fig.14*. Results shows good agreement between higher fidelity simulation and trained SVM models.

Table VI. Results for stochastic optimization of machinery configuration based on the 3 scenarios

Scenario #	Base Results [kg/m]	HFS [kg/m]	SVM Optimization [kg/m]	Difference [%]	P_{ME} [MW]	P_{PTI} [MW]	P_{Gen} [MW]	P_{Batt} [MW]
1	0.1641	0.1631	0.1627	0.6094	24.93	1.884	1.802	1.079
2	0.1500	0.1491	0.1492	0.6000	24.41	2.375	1.641	1.266
3	0.1352	0.1334	0.1339	1.331	23.93	3.554	1.239	2.606

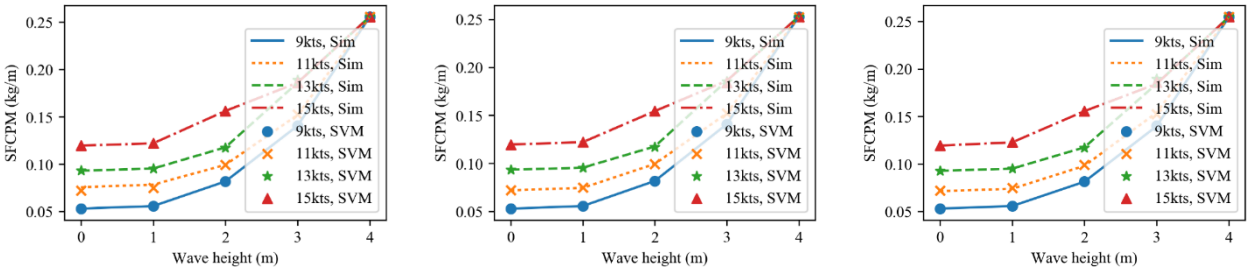

(a) Scenario 1 (b) Scenario 2 (c) Scenario 3

Fig.14: SVM prediction Vs simulation where SFCPM Vs Hs are displaced for different speeds. Results indicate very good agreement.

From optimization results performed on the metamodels in *Table VI.* for three weather scenarios, it was noted that scenario 3 has the highest potential of benefiting from finding the right design configuration with reasonable values of potential fuel savings. Also, this indicates that the trained metamodel is able to capture the behavior and fuel consumption of a complex system as a whole. Next stage is to include more degrees of freedom optimization routine from the vessel's hydrodynamic aspects such as propulsion system.

6. Conclusion

The study was set to examine the use of PIDO for hybrid marine power system design. Results indicate great potential to create a rapid design generation tool for testing multiple design alternative, sharing design constraints across subsystems and system boundaries, understanding parameters relationships between various subsystems and ultimately system level design improvements. However, unlike other aspects in ship design, hybrid marine power plant simulation is relatively new topic where tools are still developing. Therefore, after long period of testing the simulation tools for their robustness to optimization, eventually the right balance was found. Design automation and optimization has demonstrated great capability at finding many design alternatives, but well experienced engineers are needed to evaluate results as optimization algorithms work in a highly mechanistic fashion. Therefore, a combination of robust simulation tools and domain experience will assist greatly when using PIDO. Overall, DoE and RSMs demonstrated great capability of handling complex designs, decoding relationships between parameters, reducing computational cost from high fidelity multidomain models without compromising solution accuracy. Despite the design problem being highly constrained, it was possible to achieve relatively reasonable fuel saving and providing an understanding of the speed fluctuation in adverse weather conditions. Remaining work is to expand the optimization scope by including other design parameters from ship hydrodynamics and vessel operation.

Acknowledgements

The work was made possible under the assistance and PIDO software contribution from Noesis Solution in Leuven, Belgium. The author also wishes to acknowledge the contributions of his former colleagues at Noesis Solution for their technical support and for the dedication of co-author Kevin Koosup Yum who provided valuable contribution to this work.
This work is partially supported by 'Smart Maritime', a center for research based innovation (http://www.smartmaritime.no). The center is financed by the Research Council of Norway, the research partners and the industrial partners.

References

Andrews, D. (2004). "Marine Design–Requirement Elucidation rather than Requirement Engineering." Journal of Naval Engineering.

Box, G. E. and J. S. Hunter (1961). "The 2 k—p fractional factorial designs." Technometrics **3**(3): 311-351.

Box, G. E. and K. Wilson (1992). On the experimental attainment of optimum conditions. Breakthroughs in Statistics, Springer**:** 270-310.

Brereton, R. G. and G. R. Lloyd (2010). "Support vector machines for classification and regression." Analyst **135**(2): 230-267.

de Weck, O., et al. (2007). State-of-the-art and future trends in multidisciplinary design optimization. 48th Aiaa/Asme/Asce/Ahs/Asc Structures, Structural Dynamics, and Materials Conference.

Eglajs, V. and P. Audze (1977). "New approach to the design of multifactor experiments." Problems of Dynamics and Strengths **35**(1): 104-107.

Frenzel, M., et al. (2015). "Multidisciplinary optimization and integration requirements for large-scale automotive and aerospace design work."

Gero, J. S. and U. Kannengiesser (2004). "Modelling expertise of temporary design teams." Journal of Design Research **4**(3): 1-13.

Liu, Y. and M. Collette (2014). "Surrogate-assisted robust design optimization considering interval-type uncertainty." Maritime Technology and Engineering: 287-293.

Loukakis, T. and P. Sclavounos (1978). "Some extensions of the classical approach to strip theory of ship motions, including the calculation of mean added forces and moments." Journal of Ship Research **22**(1).

Parsopoulos, K. E. and M. N. Vrahatis (2002). "Recent approaches to global optimization problems through particle swarm optimization." Natural computing **1**(2-3): 235-306.

Salvesen, N., et al. (1970). "Ship motions and sea loads." Trans. SNAME **78**(8): 250-287.

Taskar, B., et al. (2016). "The effect of waves on engine-propeller dynamics and propulsion performance of ships." Ocean Engineering **122**: 262-277.

Van der Auweraer, H., et al. (2008). Breakthrough technologies for virtual prototyping of automotive and aerospace structures. Product Engineering, Springer**:** 397-418.

Yum, K. K., et al. (2016). Simulation of a Hybrid Marine Propulsion System in Waves. CIMAC Congress, CIMAC.

Yum, K. K., et al. (2016). "Simulation of a two-stroke diesel engine for propulsion in waves." International Journal of Naval Architecture and Ocean Engineering.

Annex A

Particulars of the Case Vessel and the Propulsion Plant

Propeller Geometry

Diameter (D) (m)	9.86
No of blades	4
Hub diameter (m)	1.53
Rotational speed (RPM)	95
A_e / A_0	0.431
(P/D)mean	0.47
Skew (°)	21.15
Rake (°)	0

Particulars of the main engine

Model	*Wartsila 8RT-flex68D*
Bore (mm)	680
Rated MCR (kW)	25,040
Speed at rated power (RPM)	95
Stroke (mm)	2720
Mean Effective Pressure (bar)	20
Number of cylinders	8
Turbocharger	2 x ABB A175-L35

Particulars of the electrical power plant

Number of generators	*2*
Capacity of each generator (kVA)	2000
Power factor of generator	0.9
RMS line-to-line voltage(V)	690
Number of switchboard	2
Mean hotel load during voyage (kW)	1000

Ship Particulars

Length beween perpendiculars (m)	320.0
Length at water line (m)	325.5
Breadth at water line (m)	58.0
Depth (m)	30.0
Draft (m)	20.8
Displacement (m^3)	312622
Block coefficient (C_B)	0.8098
Design Speed (m/s)	7.97

Specifications of the battery system

Energy capacity (MWh)	1.0
Maximum discharging current (kA)	5.6
Maximum charging current (kA)	5.6
Nominal voltage (V)	360

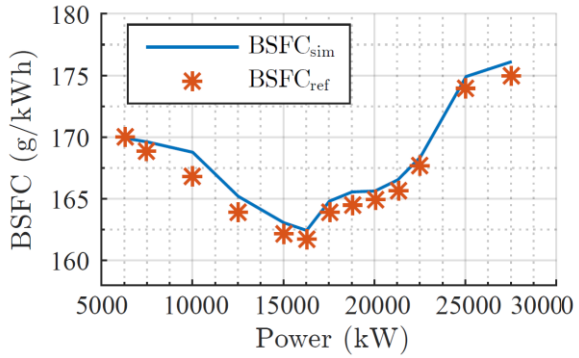

Fig.A-1: BSFC of the main engine

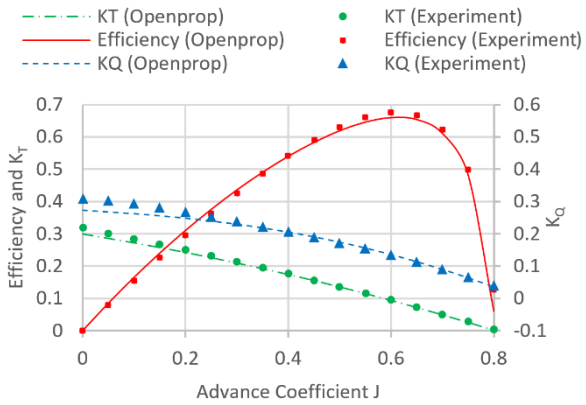

Fig.A-2: Propeller curve for the case vessel

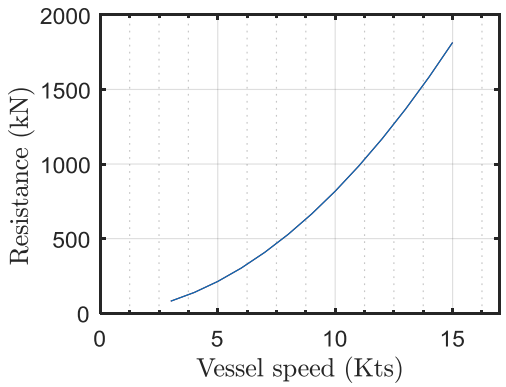

Fig.A-3: Resistance curve for the case vessel